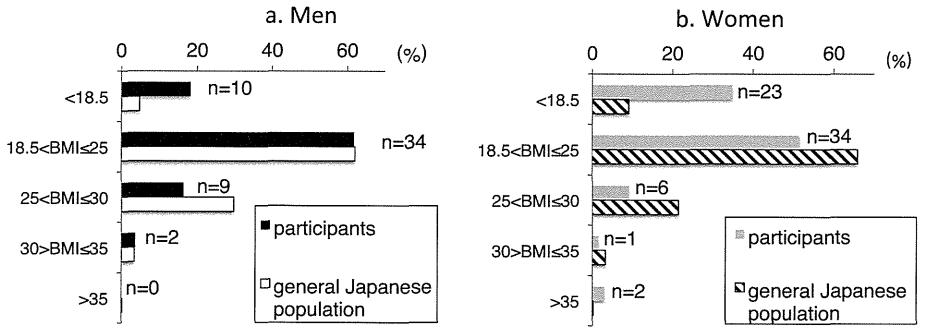

Figure 3 BMI of participants and the general adult Japanese population (aged >20 years). More registry participants were underweight compared to the general population. Proportions of underweight participants were 18.2% and 34.8% for men and women, respectively, and 4.7% and 9.1% for healthy men and women, respectively. There were fewer obese participants relative to the general population. **a.** black column: participants, open column: general Japanese population. **b.** gray column: participants, diagonal column: general Japanese population.

relationship between GNE mutations and ITP, although the underlying mechanisms are unclear and further studies would be necessary to address this issue. Of note, however, this information was obtained based on self-report by patients and/or their families. Thus, the accuracy of the diagnosis is unclear.

It is noteworthy that in some patients, initial symptoms were difficulty lifting heels, but not toes. It is conventionally thought that the initial symptom of GNE myopathy is "foot drop," as tibialis anterior muscles are strikingly affected. Our study suggests that patients whose symptoms start with calf muscle weakness may have GNE myopathy. It is also surprising that some patients had neck and finger weakness from disease onset, despite GNE myopathy being known as "distal myopathy." Thus, GNE myopathy appears to be associated with more phenotypes than expected. However, we are not confident that all patients who chose "difficulty lifting heels" exhibited prominent calf weakness in reality as well, i.e., they experienced greater calf weakness relative to tibialis anterior muscle weakness. This is one limitation of using medical histories and a registration system to collect patient data.

Although we previously reported respiratory dysfunction associated with GNE myopathy [15], 35% of participants in the present study were not examined for respiratory function, indicating that many physicians and neurologists are unaware of the clinical significance of respiratory function in the context of this disease. Although we did not observe any cases of cardiac dysfunction, it may occur in older patients or those with advanced disease. Supporting this is evidence from a study showing that 20% of GNE myopathy mice develop fibrosis in cardiac tissue after 30 weeks of age, with some exhibiting marked endomysial fibrosis, amyloid deposition, and occasionally rimmed vacuoles in cardiomyocytes [8]. This suggests that the risk of cardiopulmonary dysfunction in GNE myopathy should be considered.

In this study, four participants harbored single heterozygous mutations, although they exhibited clinicopathologically definite findings of GNE myopathy. The age at disease onset did not significantly differ between homozygotes and compound heterozygotes. Given that we limited our analysis to all exons and their flanking introns, it is possible that single heterozygotes who exhibited features of GNE myopathy may have mutations in other genomic regions of *GNE*. Yet, in the absence of data using disease-specific biomarkers, it is difficult to distinguish whether these participants had other myopathies and carried a single heterozygous mutation in the *GNE* gene.

Among registry participants, 46% were in the abnormal range of BMI, and the number of underweight participants was markedly higher in both men and women, compared to the normal population. None of the participants or patients of NCNP had dysphagia or other medical problems which might promote weight loss. The BMI of non-ambulant patients tended to be higher than ambulant patients, suggesting that muscle atrophy itself did not cause weight loss. Mechanisms underlying the weight changes may differ from those observed in muscular dystrophy such as DMD [22] or myotonic dystrophy [23], given that obesity was not an issue with most patients with GNE myopathy. It is not clear whether being underweight is beneficial relative to having normal weight in these patients. Prospective analyses will be needed to reveal the relationship between motor function prognosis and body weight.

This study has some limitations worth noting. First, we could not unify the method of grip power assessment. Second, we relied on descriptions of motor function as a crude benchmark for designing clinical trials. Finally, we could not address phenotype-genotype correlations in more depth than was previously reported [9], given the limited number of homozygote patients harboring mutations other than V572L. A larger cohort will be needed to address genotype-phenotype correlations.

Similar to our collaborations involving the dystrophinopathy registry, we are currently in discussions to harmonize the international registry of GNE myopathy of the TREAT-NMD ALLIANCE [ClinicalTrials.gov Identifier NCT01784679, http://www.treat-nmd.eu/gne/patient-registries/international-registry/] (GNE-DMP), in hopes of gaining further insights into the disease. There are two major differences between GNE-DMP. First, as the Remudy aims to establish registration according to genetic diagnosis, inclusion criteria for genetics-based longitudinal natural history studies employing the Remudy-GNE registry require genetic diagnosis (including single heterozygote). Second, we are the only Japanese language registry system. Japan has one of the largest patient groups with GNE myopathy in the world [24]. It is important that patients with this disease receive information in their native language, and that domestic information is supplied for the purpose of Japanese patient accession. Harmonisation would be conducted in order to avoid duplication and double registration of GNE patients while providing the same benefits and opportunities to patients, regardless of where they live. Both registries are similar in their processes utilized for data collection as well as their fundamental ideas regarding the registries, and thus we hope to merge the two registries at some point. According to a tentative agreement, the Remudy-GNE will remain the primary entryway into the international registry as well as serve as the contact site for Japanese patients, and only anonymous data will be stored in the joint data set. Strategies for merging the two registries are currently under consideration.

Our Japanese registry and the TREAT-MND ALLIANCE registry work in close collaboration, and will serve as irreplaceable infrastructures that accelerate research, therapy development, and trial readiness, in addition to increasing opportunities for collaboration and improving global patient care.

Conclusion

The patient registry for GNE myopathy in Japan is useful for gaining a better understanding of the disease, and recruiting patients with genetically-confirmed GNE myopathy for upcoming clinical trials. Further advances and insights can be expected through a soon-to-be-launched international GNE myopathy registry.

Additional files

Additional file 1: Table S1. Genotyping. ED = Glucosamine (UDP-N-acetyl)-2-epimerase domain, KD = N-acetylmannosamine kinase domain. There were more participants who were either homozygous for p.V572L or heterozygous for p.D176V/p.V572L compared to those with other mutations. Although p.D176V was the second most frequent mutation, there was only one participant in the registry who was homozygous for p.D176V.

Additional file 2: Table S2. Allelic frequency. p.V572L was the most frequent mutation.

Additional file 3: Figure S1. Muscle CT of 29 year-old GNE myopathy patient who reported difficulty lifting his heels as one of the first symptoms. Ankle plantar flexion (MMT 2) was prominently impaired (MMT5), and muscle CT revealed that fatty replacement and atrophy were far more prominent in the calf than the anterior part of the lower legs.

Abbreviations

GNE: Glucosamine (UDP-N-acetyl)-2-epimerase/N-acetylmannosamine kinase; NCNP: National Center of Neurology and Psychiatry; REMUDY: Registry of muscular dystrophies; DMRV: Distal myopathy with rimmed vacuoles; UDP-GlcNAc: Uridine diphosphate-*N*-acetylglucosamine; TREAT-MND ALLIANCE: Translational Research in Europe–Assessment and Treatment of Neuromuscular Diseases; SD: Standard deviation; ITP: Idiopathic thrombocytopenia; FVC: Forced vital capacity; NPPV: Non-invasive positive pressure ventilation; EF: Ejection fraction; FS: Fraction shortening; CK: Creatine kinase.

Competing interest

The authors declare that they have no competing interests.

Authors' contributions

MMY drafted/revised the manuscript, conceived of the study, participated in its design, performed data acquisition, data analysis and interpretation, and statistical analysis, and supervised the study. NY conceived of the study, participated in its design, and performed the statistical analysis. YKH drafted/revised the manuscript, performed genetic analysis, and supervised the study. IN conceived of the study, participated in its design, and carried out the genetic analysis. MM drafted /revised the manuscript and supervised the study. EK, HN, and ST conceived of the study and supervised the study. All authors read and approved the final manuscript.

Acknowledgments

We thank members of the Patients Association for Distal Myopathies in Japan (PADM). This work was partly supported by Health and Labour Sciences Research Grants for Research on Intractable Diseases, Comprehensive Research on Disability Health and Welfare Grants, Health and Labour Science Research Grants, and Intramural Research Grants (23-4/26-7) for Neurological and Psychiatric Disorders from the National Center of Neurology and Psychiatry.

Author details

[1]Department of Neurology, National Center Hospital, National Center of Neurology and Psychiatry, 4-1-1 Ogawahigashi, Kodaira, Tokyo 187-8551, Japan. [2]Department of Neuromuscular Research, National Institute of Neuroscience, National Center of Neurology and Psychiatry, 4-1-1 Ogawahigashi, Kodaira, Tokyo 187-8502, Japan. [3]Department of Neurophysiology, Tokyo Medical University, 6-1-1 Shinjuku, Shinjuku, Tokyo 160-8402, Japan. [4]Translational Medical Center, National Center of Neurology and Psychiatry, 4-1-1 Ogawahigashi, Kodaira, Tokyo 187-8551, Japan. [5]Department of Molecular Therapy, National Institute of Neuroscience, National Center of Neurology and Psychiatry, 4-1-1 Ogawahigashi, Kodaira, Tokyo 187-8502, Japan.

Received: 28 May 2014 Accepted: 16 September 2014
Published online: 11 October 2014

References

1. Nonaka I, Sunohara N, Satoyoshi E, Terasawa K, Yonemoto K: **Autosomal recessive distal muscular dystrophy: a comparative study with distal myopathy with rimmed vacuole formation.** *Ann Neurol* 1985, **17**:51–59.
2. Argov Z, Yarom R: **"Rimmed vacuole myopathy" sparing the quadriceps. A unique disorder in Iranian Jews.** *J Neurol Sci* 1984, **64**:33–43.
3. Nishino I, Noguchi S, Murayama K, Driss A, Sugie K, Oya Y, Nagata T, Chida K, Takahashi T, Takusa Y, Ohi T, Nishimiya J, Sunohara N, Ciafaloni E, Kawai M, Aoki M, Nonaka I: **Distal myopathy with rimmed vacuoles is allelic to hereditary inclusion body myopathy.** *Neurology* 2002, **59**:1689–1693.

4. Eisenberg I, Avidan N, Potikha T, Hochner H, Chen M, Olender T, Barash M, Shemesh M, Sadeh M, Grabov-Nardini G, Shmilevich I, Friedmann A, Karpati G, Bradley WG, Baumbach L, Lancet D, Asher EB, Beckmann JS, Argov Z, Mitrani-Rosenbaum S: **The UDP-N-acetylglucosamine 2-epimerase/N-acetylmannosamine-kinase gene is mutated in recessive hereditary inclusion body myopathy.** *Nat Genet* 2001, **29**:83–87.
5. Kayashima T, Matsuo H, Satoh A, Ohta T, Yoshiura K, Matsumoto N, Nakane Y, Niikawa N, Kishino T: **Nonaka myopathy is caused by mutations in the UDP-N-acetylglucosamine-2-epimerase/N-acetylmannosamine kinase gene (GNE).** *J Hum Genet* 2002, **47**:77–79.
6. Keppler OT, Hinderlich S, Langner J, Schwartz-Albiez R, Reutter W, Pawlita M: **UDP–GlcNAc 2-epimerase: a regulator of cell surface sialylation.** *Science* 1999, **284**:1372–1376.
7. Malicdan MC, Noguchi S, Nishino I: **Recent advances in distal myopathy with rimmed vacuoles (DMRV) or hIBM: treatment perspectives.** *Curr Opin Neurol* 2008, **21**:596–600.
8. Malicdan MC, Noguchi S, Hayashi YK, Nonaka I, Nishino I: **Prophylactic treatment with sialic acid metabolites precludes the development of the myopathic phenotype in the GNE myopathy mouse model.** *Nat Med* 2009, **15**:690–695.
9. Cho A, Hayashi YK, Monma K, Oya Y, Noguchi S, Nonaka I, Nishino I: **Mutation profile of the GNE gene in Japanese patients with distal myopathy with rimmed vacuoles (GNE myopathy).** *J Neurol Neurosurg Psychiatry* 2013, **11**. doi: 10.1136/jnnp-2013-305587. [Epub ahead of print].
10. Richesson R, Vehik K: **Patient registries: utility, validity and inference.** *Adv Exp Med Biol* 2010, **686**:87–104.
11. Bladen CL, Rafferty K, Straub V, Monges S, Moresco A, Dawkins H, Roy A, Chamova T, Guergueltcheva V, Korngut L, Campbell C, Dai Y, Barišić N, Kos T, Brabec P, Rahbek J, Lahdetie J, Tuffery-Giraud S, Claustres M, Leturcq F, Ben Yaou R, Walter MC, Schreiber O, Karcagi V, Herczegfalvi A, Viswanathan V, Bayat F, de la Caridad Guerrero Sarmiento I, Ambrosini A, Ceradini F, *et al*: **The TREAT-NMD Duchenne muscular dystrophy registries: conception, design, and utilization by industry and academia.** *Hum Mutat* 2013, **34**:1449–1457.
12. *TREAT-MND ALLIANCE.* website. [http://www.treat-nmd.eu.].
13. Nakamura H, Kimura E, Mori-Yoshimura M, Komaki H, Matsuda Y, Goto K, Hayashi YK, Nishino I, Takeda SI, Kawai M: **Characteristics of Japanese Duchenne and Becker muscular dystrophy patients in a novel Japanese national registry of muscular dystrophy (Remudy).** *Orphanet J Rare Dis* 2013, **19**:60.
14. Takeuchi F, Yonemoto N, Nakamura H, Shimizu R, Komaki H, Mori-Yoshimura M, Hayashi YK, Nishino I, Kawai M, Kimura E, Takeda S: **Prednisolone improves walking in Japanese Duchenne muscular dystrophy patients.** *J Neurol* 2013, **260**:3023–3029.
15. Mori-Yoshimura M, Monma K, Suzuki N, Aoki M, Kumamoto T, Tanaka K, Tomimitsu H, Nakano S, Sonoo M, Shimizu J, Sugie K, Nakamura H, Oya Y, Hayashi YK, Malicdan MC, Noguchi S, Murata M, Nishino I: **GNE myopathy (Distal myopathy with rimmed vacuoles) patients with mutations in the UDP-GlcNAc 2-epimerase and in the *N*-acetylmannosamine kinase domains of the *GNE* gene exhibit less severe phenotypes than patients with mutations only in MNK domain.** *J Neurol Sci* 2012, **15**:100–105.
16. Mori-Yoshimura M, Oya Y, Hayashi YK, Noguchi S, Nishino I, Murata M: **Respiratory dysfunction in patients severely affected by GNE myopathy (distal myopathy with rimmed vacuoles).** *Neuromuscul Disord* 2013, **23**:84–8.
17. Mori-Yoshimura M, Oya Y, Yajima H, Yonemoto N, Kobayashi Y, Hayashi YK, Noguchi S, Nishino I, Murata M: **GNE myopathy: a prospective natural history study of disease progression.** *Neuromuscul Disord* 2014, **24**:380–386.
18. Mori A: **Obesity guideline committee, Guideline for diagnosis and therapy of Obesity.** *Obesity J Japan Soc Study Obesity* 2011, **17**(suppl):1–10 [in Japanese].
19. *UMIN CTR.* website. [https://upload.umin.ac.jp/cgi-open-bin/ctr/ctr.cgi?function=brows&action=brows&type=summary&recptno=R000013489&language=J].
20. *Japan intractable Diseases Information Center Homepage.* [http://www.nanbyou.or.jp/entry/157].
21. Crook M, Machin S, Crawford N: **Electrokinetic behaviour and surface sialic acid status of blood platelets in essential thrombocythaemia (ET).** *Eur J Haematol* 1992, **49**:128–132.
22. Leung DG, Germain-Lee EL, Denger BE, Wagner KR: **Report on the Second Endocrine Aspects Of Duchenne Muscular Dystrophy Conference December 1–2, 2010, Baltimore, Maryland, USA.** *Neuromuscul Disord* 2011, **21**:594–601.
23. Gagnon C, Chouinard MC, Laberge L, Brisson D, Gaudet D, Lavoie M, Leclerc N, Mathieu J: **Prevalence of lifestyle risk factors in myotonic dystrophy type 1.** *Can J Neurol Sci* 2013, **40**:42–47.
24. Nishino I, Carrillo-Carrasco N, Argov Z: **GNE myopathy: current update and future therapy.** *J Neurol Neurosurg Psychiatry* 2014, doi: 10.1136/jnnp-2013-307051. [Epub ahead of print] Review.

doi:10.1186/s13023-014-0150-4
Cite this article as: Mori-Yoshimura *et al.*: Nationwide patient registry for GNE myopathy in Japan. *Orphanet Journal of Rare Diseases* 2014 **9**:150.

Goto et al. Orphanet Journal of Rare Diseases 2014, 9:58
http://www.ojrd.com/content/9/1/58

ORPHANET JOURNAL OF RARE DISEASES

RESEARCH Open Access

A nationwide survey on Marinesco-Sjögren syndrome in Japan

Masahide Goto[1,2], Mari Okada[3], Hirofumi Komaki[1], Kenji Sugai[1], Masayuki Sasaki[1], Satoru Noguchi[3,4], Ikuya Nonaka[3], Ichizo Nishino[3,4] and Yukiko K Hayashi[3,4,5*]

Abstract

Background: Marinesco-Sjögren syndrome (MSS) is an autosomal recessive multisystem disorder characterized by the tetralogy of cerebellar ataxia, congenital cataracts, intellectual disability, and progressive muscle weakness due to myopathy. MSS is extremely rare, and its clinical, pathological, and genetic features are not yet fully understood.

Methods: We conducted a nationwide, questionnaire-based survey on MSS in Japan and carefully reviewed the medical records of 36 patients suspected of having this disease. In addition, pathological examinations of muscles, sequence and haplotype analysis in *SIL1* were performed.

Results: The patients had been examined between the ages of 2 and 52 years. Delayed psychomotor development and cataracts from early childhood were observed in all patients, whereas no life-threatening events were observed. Mutations in *SIL1* were identified in 24 of the 27 patients tested, and 43 of the 48 chromosomes possessed the *SIL1* c.936dupG (p.Leu313fs) mutation. The haplotype analysis revealed that 31 of the 32 chromosomes (96.9%) with the c.936dupG mutation had the same haplotype.

Conclusions: The results of haplotype analysis suggested the presence of a founder effect. The clinical features of patients without *SIL1* mutations were indistinguishable from those with *SIL1* mutations, suggesting the genetic heterogeneity of MSS.

Keywords: Marinesco-Sjögren syndrome (MSS), *SIL1*, Founder effect, Cataracts, Intellectual disability, Ataxia, Rimmed vacuolar myopathy

Background

Marinesco-Sjögren syndrome (MSS; OMIM 248800) is an autosomal recessive multisystem disorder clinically characterized by the tetralogy of cerebellar ataxia, congenital cataracts, intellectual disability, and progressive muscle weakness due to myopathy [1-3]. Additional clinical features, including short stature, hypergonadotropic hypogonadism [4], and strabismus [5], are also observed. Mutations in *SIL1* (Gene ID: 64374) were reported to be causative for MSS [6,7]. This gene encodes SIL1, also known as BiP-associated protein (BAP), which is an endoplasmic reticulum (ER)-resident protein. Bip is an HSP70 chaperone family member located in the ER, and plays a key role in protein quality control. SIL1 regulates the ATPase cycle of BiP for proper protein folding [8,9]. SIL1-deficient woozy mutant mice exhibit progressive ataxia caused by the loss of Purkinje cells via ER stress [10].

MSS is an extremely rare disease, and very few cases have been reported. In this study, we performed a nationwide, questionnaire-based survey on MSS with the aim of characterizing its prevalence, clinical features, natural history, muscle pathological findings, and mutation status.

Methods

All clinical materials used in this study were obtained for diagnostic purposes with written informed consent. All surveys and experiments performed in this study were approved by the Ethical Committee of the National Center of Neurology and Psychiatry.

* Correspondence: yhayashi@tokyo-med.ac.jp
[3]Department of Neuromuscular Research, National Institute of Neuroscience, National Center of Neurology and Psychiatry, Tokyo, Japan
[4]Department of Clinical Development, Translational Medical Center, National Center of Neurology and Psychiatry, Tokyo, Japan
Full list of author information is available at the end of the article

The nationwide, questionnaire-based survey

To elucidate the clinical characteristics of MSS, we conducted a nationwide, questionnaire-based survey in Japan. The first set of questionnaires, which focused on the experience of treating patients suspected of having MSS, was sent to a total of 5,452 Japanese specialists for neurology or pediatric neurology. The second set of questionnaires, which focused on the clinical information of patients with suspected MSS, was sent to their attending physicians. These patients' medical records were carefully reviewed by 2 of our specialists (M.G., H.K.).

Histochemistry

Biopsied muscle specimens were flash-frozen in isopentane cooled in liquid nitrogen. Transverse serial frozen sections of 10 μm in thickness were subjected to various types of histochemical staining, including hematoxylin and eosin (H&E), modified Gomori-trichrome (mGT), and ATPases. We obtained biopsied skeletal muscles from a total of 17 unrelated patients clinically suspected of having MSS.

Sequence analysis of *SIL1*

Genomic DNA was extracted from either frozen muscle or peripheral blood lymphocytes using standard protocols. The PCR primers were designed to amplify all the exons of *SIL1* together with their flanking intronic regions. The primer sequences are available upon request. Direct sequencing was performed using the BigDye Terminator v3.1 Cycle Sequencing system and an ABI3100 automated Genetic Analyzer (Applied Biosystems, Foster City, CA). The sequence data obtained were analyzed using the SeqScape (Applied Biosystems) program and compared with the genomic sequence of *SIL1* in the database (NM_022464). Genetic analysis was performed on DNA from 27 unrelated patients and the parents of 3 of them. Two hundred control chromosomes from healthy individuals were examined for each novel mutation in *SIL1* by direct sequencing.

Haplotype analysis of *SIL1*

For the haplotype analysis of the *SIL1* genomic region, we performed direct sequencing of the following 11 common single nucleotide variants (SNVs) in the Japanese population: rs11748097, rs929775, rs10045761, rs1433008, rs1 1958050, rs7717375, rs7722413, rs3763016, rs6596456, rs700629, and rs12653845 (http://www.ncbi.nlm.nih.gov/SNP/). Samples from 21 patients homozygous for the common c.936dupG mutation, the parents of 3 patients, and 92 control Japanese individuals were analyzed.

Results

Patients

A total of 1,875 responses (34.4% response rate) were received to the first set of questionnaires. The second set of questionnaires was sent to a total of 37 attending physicians (2.0%) who had treated patients suspected of having MSS. The detailed clinical records of a total of 36 patients were carefully reviewed. The shortfall in the number of patients was due to an overlap of 1 case.

Sequence analysis of *SIL1*

Frozen muscle or peripheral blood lymphocytes were obtained from 27 of the 36 patients suspected of having MSS, for genetic analysis. Mutations in *SIL1* were identified in 24 out of the 27 patients. Twenty-one patients were homozygous for the previously reported c.936dupG (p.Leu313fs) mutation in exon 9. Patient 4 was homozygous for the previously reported c.603_607del5 (p.Glu201fs) mutation in exon 6 [11]. Patient 12 was homozygous for the previously reported c.331C > T (p.Arg111X) mutation in exon 4 [6,7]. Patient 17 was a compound heterozygote for the novel c.617_618TC > AA (p.Leu206Glu) mutation in exon 6 and the c.936dupG (p.Leu313fs) mutation in exon 9 [12]. All mutations except for p.Leu206Glu are predicted to induce premature termination. Mutation of Leu206, which is highly conserved among species, was predicted to exert a deleterious impact on protein function by the Polymorphism Phenotyping v2 (PolyPhen-2; http://genetics.bwh.harvard.edu/pph2/) and the Sorting Intolerant From Tolerant software (SIFT: http://sift.bii.a-star.edu.sg/). None of these nucleic acid changes were found in the 200 chromosomes from healthy Japanese controls or in the Japanese Single Nucleotide Polymorphisms database (http://snp.ims.u-tokyo.ac.jp/index_ja.html).

Haplotype analysis of *SIL1*

The *SIL1* c.936dupG mutation was identified in 43 of the 48 chromosomes (89.6%) in our cohort. The patients carrying this mutation were reported from different areas in Japan. To determine whether this was a result of a founder effect, we performed a haplotype analysis using 11 SNVs within or close to *SIL1*. The results revealed that 31 of the 32 chromosomes (96.9%) with the c.936dupG mutation had the same haplotype (P1-P24, Table 1). This haplotype was only found in 18 of the 184 chromosomes (9.8%) from the control group, suggesting a founder effect, although 1 chromosome from Patient 1 had a different haplotype.

Clinical features

Table 2 and Additional file 1: Table S1 show a clinical summary of the patients in our series.

The age at which the examination was performed in the 24 patients (10 men and 14 women) with *SIL1* mutations varied from 2 to 52 (mean = 20.1 ± 18.1) years. Bilateral cataracts requiring prompt surgical intervention had appeared and rapidly progressed in all 24 patients at the mean age of 3.5 ± 1.2 years. Strabismus was also

Table 1 Haplotype analysis

rs No	rs11748097	rs929775	rs10045761	*/#	rs1433008	rs11958050	rs7717375	@	rs7722413	rs3763016	rs6596456	rs700629	rs12653845
JPT	A: 0.24	G: 0.18	A: 0.15		C: 0.15	A: 0.76	A: 0.82		C: 0.11	G: 0.11	A: 0.13	A: 0.14	G: 0.11
P1	C/A	T/G	G	N	T	A/G	A	H	T/C	C/G	A	A	T
P2	C	T	G	N	T	A	A	H	T	C	A	A	T
P3	C	T	G	N	T	A	A	H	T	C	A	A	T
P5	C	T	G	N	T	A	A	H	T	C	A	A	T
P6	C	T	G	N	T	A	A	H	T	C	A	A	T
P7	C	T	G	N	T	A	A	H	T	C	A	A	T
P9	C	T	G	N	T	A	A	H	T	C	A	A	T
P10	C	T	G	N	T	A	A	H	T	C	A	A	T
P13	C	T	G	N	T	A	A	H	T	C	A	A	T
P14	C	T	G	N	T	A	A	H	T	C	A	A	T
P15	C	T	G	N	T	A	A	H	T	C	A	A	T
P16	C	T	G	N	T	A	A	H	T	C	A	A	T
P18	C	T	G	N	T	A	A	H	T	C	A	A	T
P20	C	T	G	N	T	A	A	H	T	C	A	A	T
P21	C	T	G	N	T	A	A	H	T	C	A	A	T
P24	C	T	G	N	T	A	A	H	T	C	A	A	T
P12	C	T	G	*	T	A	A	N	T	C	A	A	T
P4	C	T	G	#	T	A	A	N	T	C	G	C	T
P25	C/A	T/G	G/A	N	T/C	A/G	A/G	N	T	C	G	C	T/G
P26	C/A	T/G	G/A	N	T/C	A/G	A/G	N	T	C	G	C	T/G
P27	C	T	G	N	T	A	A	N	T	C	G	C	T

@: c.936dupG, *: c.331C > T, #: c.603_607del, JPT: Japanese frequency.
N: Normal, H: Homozygous.

Table 2 Clinical summary of patients

SIL1 mutations			Positive (n = 24)	Negative (n = 3)	Not examined (n = 9)
Ocular involvements		Cataracts	24/24 (100%), 2y-6y	3/3 (100%)	9/9 (100%)
		Strabismus	10/18 (56%)	1/3 (33%)	5/7 (71%)
		Muscle weakness	21/22 (95%), 2y-52y	3/3 (100%)	9/9 (100%)
Motor functions	Development	Head control	21/21 (100%), 4 m-18 m	5 m-8 m	4 m-7 m
		Sit	20/20 (100%), 10 m-36 m	12 m-18 m	12 m-36 m
		Stand with support	16/20 (80%), 1y-4y	15 m, 24 m	15 m-6y
		Walk with support	16/20 (80%), 2y-22y	2/2 (100%) 15 m, 24 m	3/3 (100%) 15 m-6y
		Loss of ambulation	5/16, 13y-28y		
Cerebellar signs		Hypotonia	21/24 (88%)	3/3 (100%)	9/9 (100%)
		Ataxia	16/24 (67%), 2y-52y	2/3 (100%)	6/8 (75%)
		Nystagmus	11/24 (46%), 2y-45y	0/3	5/8 (63%)
		Dysarthria	8/24 (33%), 2y-48y	2/3 (67%)	4/9 (44%)
	Psychomotor delay		20/22 (91%), IQ(DQ):24-100	3/3 (100%)	9/9 (100%)
	Hypogonadism		3/8 (38%)	0/1	2/3 (67%)
Skeletal abnormalities		Short stature	12/18 (67%),	1/3 (33%)	3/8 (38%)
		Spinal deformities	8/22 (36%)	1/3 (33%)	3/7 (43%)
		Flat foot	7/22 (32%)	0/3	1/7 (14%)
		Short fingers	5/22 (23%)	0/3	2/8 (25%)
Others		Serum CK (IU/L)	28-2000	144-3010	95-600
		Cerebellar atrophy	19/19 (100%)	3/3 (100%)	9/9(100%)
		Rimmed vacuoles in muscles	16/16 (100%)	0/1	2/6 (33%)

observed in 55.6% (10/18) of the patients. Cerebellar signs included hypotonia (21/24; 88%), ataxia (16/24; 67%), nystagmus (11/24; 46%), and dysarthria (8/24; 33%) were seen. Brain MRI demonstrated marked atrophy of the cerebellum, particularly the vermis, in all the patients examined (19/19). Mild to moderate intellectual disability, diagnosed by intelligence quotient/developmental quotient between 35 and 70, was seen in 91% (20/22) of the patients. Acquisition of meaningful words occurred at the age of 2.0 ± 0.8 years, and most of the patients had required special-needs education. Muscle weakness was observed in 95% (21/22) of the patients, with delays in motor milestones. Head control was first seen in all the patients at a certain time point between 4 and 18 (mean = 7.8 ± 3.7) months, and sitting at a certain time point between 10 and 36 (mean = 20.0 ± 8.7) months. Eighty percent (16/20) of the patients could stand with support at a certain point between the ages of 1 and 4 years, and walk with support at a certain point between the ages of 2 and 22 (mean = 5.8 ± 2.6) years; however, none of the patients acquired the ability to walk independently. Muscle weakness was slowly progressive and predominantly in the proximal muscles, with the patients becoming wheelchair-bound at a certain time point between the ages of 13 and 28 (mean = 17.4 ± 6.3) years. Serum creatine kinase levels were normal to moderately elevated (28–2000, mean = 389 ± 464; normal < 200 IU/L). Short stature (< −2 SD) was seen in 67% (12/18, mean = −3.6 SD) of the patients, and spinal deformity (8/22; 36%), flat foot (7/22; 32%), and short fingers (5/22; 23%) were also reported. Hypogonadotropic hypogonadism was seen in 3 of 8 (38%) patients (1 with microtestis, 2 with amenorrhea). No marked clinical differences were observed among patients with different *SIL1* mutations. No patient had cardiac and respiratory problems.

The 3 patients with no *SIL1* mutation (Patients 25, 26, and 27) and the 9 genetically unexamined patients showed clinical features indistinguishable from the patients with *SIL1* mutations, including cerebellar signs with cerebellar atrophy on brain images, intellectual disability, congenital cataracts, and muscle weakness. Elevation of serum CK levels was also seen in 2 patients (Table 2).

Pathological findings of skeletal muscles

Biopsied skeletal muscles were obtained from 16 patients with *SIL1* mutations and one patient without (Patient 27). All muscle specimens showed myopathic changes of variation in fiber size and endomysial fibrosis. A few necrotic and regenerating fibers were seen in some patients with *SIL1* mutations. No neurogenic changes, including fiber type grouping and grouped atrophy, were observed in any of the patients. Importantly, scattered rimmed vacuoles (RVs) were seen in all 16 patients with *SIL1* mutations, but not in the patient without (Figure 1).

Discussion

We conducted a nationwide, questionnaire-based survey to clarify the prevalence, clinical and pathological characteristics, and long-term course of MSS in Japanese patients. The total number of patients with MSS was only 36.

From a clinical point of view, it is important to carry out careful ophthalmological examination of MSS patients at a young age if visual acuity is to be preserved, as the cataracts characteristic of MSS usually appear abruptly and develop rapidly from an early age [13,14]. Indeed, all of the patients in our present series required early and prompt surgical intervention. Marked cerebellar atrophy on brain MRI is another characteristic of this disease, however cerebellar ataxia can be difficult to identify, especially in younger patients with muscle weakness. Skeletal muscle weakness is also a prominent characteristic. Almost all the MSS patients with *SIL1* mutations in this series had muscle weakness initially noticed as a delayed motor milestone, which was detected at an earlier age than cataracts, as reported previously [3,15,16]. Regarding muscle biopsy, myopathic changes, including RV formation are a characteristic of patients with *SIL1* mutations. RVs are not disease-specific, and are often seen in adult-onset chronic myopathies such as inclusion body myositis,

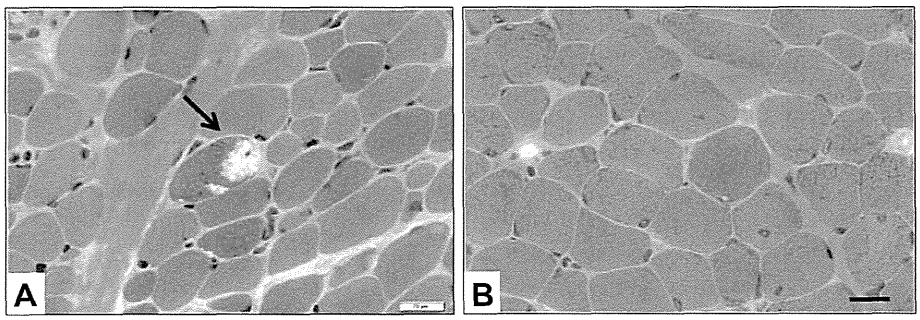

Figure 1 Modified gomori trichrome stain of the biopsied skeletal muscles. A muscle from a MSS patient with *SIL1* mutation shows rimmed vacuoles (arrow, **A**), whereas no vacuole is seen in a patient without *SIL1* mutation (**B**). Bar = 20 μm.

distal myopathy with RVs, oculopharyngeal muscular dystrophy, and myofibrillar myopathies. They are rarely observed, however, in childhood-onset myopathies. The presence of RVs in muscle biopsy tissue can be helpful in formulating an early diagnosis of MSS, allowing the ophthalmologist to perform surgery for cataracts to prevent total visual loss. The life prognosis of MSS appears to be comparatively good, as respiratory, cardiac, and swallowing functions are well preserved, even in the patients who are over 50 years of age.

Most of the reported *SIL1* gene mutations have been predicted to induce premature termination and loss of function of SIL1. Based on a putative model of SIL1-BiP interaction, the C-terminal 5 amino acids of SIL1 are thought to play a key role in its association with BiP [17]. This concept is further strengthened by the fact that the p.Arg111X, p.Glu201fs, and p.Leu313fs mutations cause the generation of SIL1 proteins lacking the C-terminal region. Complete loss of function due to nonsense-mediated mRNA decay should also be considered. On the other hand, Leu206 in exon 6 is well preserved among species, and the novel nonsynonymous mutation p.Leu206Glu is predicted to exert a deleterious impact on protein function by both SIFT and PolyPhen2. The c.936dupG (p.Leu313fs) mutation in *SIL1*, which was first reported from Japan [12], is highly common in Japanese MSS patients. Haplotype analysis revealed that whereas 96.9% of chromosomes from MSS patients possessing the c.936dupG mutation had the same haplotype, less than 10% of the chromosomes of the controls did so, suggesting a founder effect.

The results of this study also strongly suggest the genetic heterogeneity of MSS. Three of the 27 patients (11.1%) had no *SIL1* mutation, but demonstrated the cardinal features of MSS, including congenital cataracts, ataxia, intellectual disability, and myopathy. We could not exclude the possibility of the mutation occurred in the promoter or other non-coding region of *SIL1* in these 3 patients. Previous reports also showed that approximately one-half of the MSS patients were genetically diagnosed as MSS from mutations in *SIL1* [7,16]. The absence of RVs in the muscle biopsy tissue of one patient with no *SIL1* mutation suggests the existence of a different disease mechanism(s) in such patients. Further analysis is required to identify the other causative genes for MSS.

Conclusions

MSS is an extremely rare disease, but a possible founder effect was present in Japan. The life prognosis of MSS is comparatively good, and early diagnosis is important for prevention of a total visual loss. Other causative genes for MSS can cause indistinguishable clinical features via different disease mechanisms.

Additional file

Additional file 1: Table S1. Clinical findings of each patient with or without *SIL1* mutations.

Competing interests

The authors declare that they have no competing of interest.

Authors' contributions

MG had full access to all the data in the study and wrote the manuscript; MO performed the mutation analysis; HK participated in analyzing all the clinical data; KS, MS, SN, I Nonaka, and I Nishino were involved in data interpretation and also supervised manuscript preparation. YKH supervised all aspects of the study, including study design, data interpretation, and manuscript preparation. All authors read and approved the final manuscript.

Acknowledgements

The authors would like to thank Kanako Goto and Maki Takami for their invaluable technical support and assistance with the genetic analysis. The authors also thank Jeremy Williams (MA, Professor), Dr. Helena Popiel (MS, PhD, Lecturer), and Dr. Edward Barroga (DVM, PhD, Associate Professor) of the Department of International Medical Communications of Tokyo Medical University for editing and reviewing the manuscript.

Funding

This study was supported partly by grants for Research on Intractable Diseases, Comprehensive Research on Disability Health and Welfare, and Applying Health Technology, from the Ministry of Health, Labour and Welfare, Japan; partly by Intramural Research Grants 23–4, 23–5, 22–5 for Neurological and Psychiatric Disorders from the National Center of Neurology and Psychiatry; and partly by JSPS KAKENHI Grant Numbers 23390236 and 24390227.

Author details

[1]Department of Child Neurology, National Center Hospital, National Center of Neurology and Psychiatry, Tokyo, Japan. [2]Department of Pediatrics, Hitachiomiya Saiseikai Hospital, Ibaraki, Japan. [3]Department of Neuromuscular Research, National Institute of Neuroscience, National Center of Neurology and Psychiatry, Tokyo, Japan. [4]Department of Clinical Development, Translational Medical Center, National Center of Neurology and Psychiatry, Tokyo, Japan. [5]Department of Neurophysiology, Tokyo Medical University, Tokyo, Japan.

Received: 12 December 2013 Accepted: 14 April 2014
Published: 23 April 2014

References

1. Sjogren T: **Hereditary congenital spinocerebellar ataxia accompanied by congenital cataract and oligophrenia; a genetic and clinical investigation.** *Confin Neurol* 1950, **10**:293–308.
2. Herva R, von Wendt L, von Wendt G, Saukkonen AL, Leisti J, Dubowitz V: **A syndrome with juvenile cataract, cerebellar atrophy, mental retardation and myopathy.** *Neuropediatrics* 1987, **18**:164–169.
3. Superneau DW, Wertelecki W, Zellweger H, Bastian F: **Myopathy in marinesco-sjogren syndrome.** *Eur Neurol* 1987, **26**:8–16.
4. Skre H, Berg K: **Linkage studies on marinesco-sjogren syndrome and hypergonadotropic hypogonadism.** *Clin Genet* 1977, **11**:57–66.
5. Dotti MT, Bardelli AM, De Stefano N, Federico A, Malandrini A, Vanni M, Guazzi GC: **Optic atrophy in marinesco-sjogren syndrome: an additional ocular feature: report of three cases in two families.** *Ophthalmic Paediatr Genet* 1993, **14**:5–7.
6. Anttonen AK, Mahjneh I, Hamalainen RH, Lagier-Tourenne C, Kopra O, Waris L, Anttonen M, Joensuu T, Kalimo H, Paetau A, Tranebjaerg L, Chaigne D, Koenig M, Eeg-Olofsson O, Udd B, Somer M, Somer H, Lehesjoki AE: **The gene disrupted in marinesco-sjogren syndrome encodes SIL1, an HSPA5 cochaperone.** *Nat Genet* 2005, **37**:1309–1311.
7. Senderek J, Krieger M, Stendel C, Bergmann C, Moser M, Breitbach-Faller N, Rudnik-Schöneborn S, Blaschek A, Wolf NI, Harting I, North K, Smith J, Muntoni F, Brockington M, Quijano-Roy S, Renault F, Herrmann R, Hendershot LM, Schröder JM, Lochmüller H, Topaloglu H, Voit T, Weis J, Ebinger F, Zerres K:

Mutations in SIL1 cause marinesco-sjogren syndrome, a cerebellar ataxia with cataract and myopathy. *Nat Genet* 2005, **37**:1312–1314.
8. Zoghbi HY: **SILencing misbehaving proteins.** *Nat Genet* 2005, **37**:1302–1303.
9. Shomura Y, Dragovic Z, Chang HC, Tzvetkov N, Young JC, Brodsky JL, Guerriero V, Hartl FU, Bracher A: **Regulation of Hsp70 function by HspBP1: structural analysis reveals an alternate mechanism for Hsp70 nucleotide exchange.** *Mol Cell* 2005, **17**:367–379.
10. Zhao L, Longo-Guess C, Harris BS, Lee JW, Ackerman SL: **Protein accumulation and neurodegeneration in the woozy mutant mouse is caused by disruption of SIL1, a cochaperone of BiP.** *Nat Genet* 2005, **37**:974–979.
11. Takahata T, Yamada K, Yamada Y, Ono S, Kinoshita A, Matsuzaka T, Yoshiura K, Kitaoka T: **Novel mutations in the SIL1 gene in a Japanese pedigree with the marinesco-sjögren syndrome.** *J Hum Genet* 2010, **55**:142–146.
12. Eriguchi M, Mizuta H, Kurohara K, Fujitake J, Kuroda Y: **Identification of a new homozygous frameshift insertion mutation in the SIL1 gene in 3 Japanese patients with marinesco-sjogren syndrome.** *J Neurol Sci* 2008, **270**:197–200.
13. Ishikawa T, Kitoh H, Awaya A, Nonaka I: **Rapid cataract formation in marinesco-sjogren syndrome.** *Pediatr Neurol* 1993, **9**:407–408.
14. Shimizu T, Matsuishi T, Yamashita Y, Koga Y, Ohtaki E, Kato H, Goto Y, Nonaka I: **Marinesco-sjogren syndrome: can the diagnosis be made prior to cataract formation?** *Muscle Nerve* 1997, **20**:909–910.
15. Horvers M, Anttonen AK, Lehesjoki AE, Morava E, Wortmann S, Vermeer S, van de Warrenburg BP, Willemsen MA: **Marinesco-sjogren syndrome due to SIL1 mutations with a comment on the clinical phenotype.** *Eur J Paediatr Neurol* 2013, **17**:199–203.
16. Krieger M, Roos A, Stendel C, Claeys KG, Sonmez FM, Baudis M, Bauer P, Bornemann A, de Goede C, Dufke A, Finkel RS, Goebel HH, Häussler M, Kingston H, Kirschner J, Medne L, Muschke P, Rivier F, Rudnik-Schöneborn S, Spengler S, Inzana F, Stanzial F, Benedicenti F, Synofzik M, Lia Taratuto A, Pirra L, Tay SK, Topaloglu H, Uyanik G, *et al*: **SIL1 mutations and clinical spectrum in patients with marinesco-sjogren syndrome.** *Brain* 2013, **136**:3634–3644.
17. Howes J, Shimizu Y, Feige MJ, Hendershot LM: **C-terminal mutations destabilize SIL1/BAP and can cause marinesco-sjogren syndrome.** *J Biol Chem* 2012, **287**:8552–8560.

doi:10.1186/1750-1172-9-58
Cite this article as: Goto *et al.*: A nationwide survey on Marinesco-Sjögren syndrome in Japan. *Orphanet Journal of Rare Diseases* 2014 **9**:58.

Available online at www.sciencedirect.com

ScienceDirect

Neuromuscular Disorders 25 (2015) 60–69

www.elsevier.com/locate/nmd

Congenital myasthenic syndrome in Japan: Ethnically unique mutations in muscle nicotinic acetylcholine receptor subunits

Yoshiteru Azuma [a,b], Tomohiko Nakata [a,b], Motoki Tanaka [c], Xin-Ming Shen [d], Mikako Ito [a], Satoshi Iwata [a], Tatsuya Okuno [a], Yoshiko Nomura [e], Naoki Ando [f], Keiko Ishigaki [g], Bisei Ohkawara [a], Akio Masuda [a], Jun Natsume [b], Seiji Kojima [b], Masahiro Sokabe [c], Kinji Ohno [a,*]

[a] *Division of Neurogenetics, Center for Neurological Diseases and Cancer, Nagoya University Graduate School of Medicine, Nagoya, Japan*
[b] *Department of Pediatrics, Nagoya University Graduate School of Medicine, Nagoya, Japan*
[c] *Department of Physiology, Nagoya University Graduate School of Medicine, Nagoya, Japan*
[d] *Department of Neurology, Mayo Clinic, Rochester, MN, USA*
[e] *Segawa Neurological Clinic for Children, Tokyo, Japan*
[f] *Department of Pediatrics, Nagoya City University Graduate School of Medicine, Nagoya, Japan*
[g] *Department of Pediatrics, Tokyo Women's Medical University, Tokyo, Japan*

Received 29 May 2014; received in revised form 9 August 2014; accepted 3 September 2014

Abstract

Congenital myasthenic syndromes (CMS) are caused by mutations in genes expressed at the neuromuscular junction. Most CMS patients have been reported in Western and Middle Eastern countries, and only four patients with *COLQ* mutations have been reported in Japan. We here report six mutations in acetylcholine receptor (AChR) subunit genes in five Japanese patients. Five mutations are novel, and one mutation is shared with a European American patient but with a different haplotype. Among the observed mutations, p.Thr284Pro (p.Thr264Pro according to the legacy annotation) in the epsilon subunit causes a slow-channel CMS. Five other mutations in the delta and epsilon subunits are splice site, frameshift, null, or missense mutations causing endplate AChR deficiency. We also found a heteroallelic p.Met465Thr in the beta subunit in another patient. p.Met465Thr, however, was likely to be polymorphism, because single channel recordings showed mild shortening of channel openings without affecting cell surface expression of AChR, and the minor allelic frequency of p.Met465Thr was 5.1% in the Japanese population. Lack of shared mutant alleles between the Japanese and the other patients suggests that most mutations described here are ethnically unique or *de novo* in each family.

Keywords: Congenital myasthenic syndromes; Acetylcholine receptor; Slow channel syndrome; Fast channel syndrome; Endplate acetylcholine receptor deficiency

1. Introduction

Acetylcholine released from the nerve terminal binds to muscle nicotinic acetylcholine receptor (AChR) at the motor endplate. AChR is clustered at the neuromuscular junction (NMJ) by binding to rapsyn with a stoichiometry of rapsyn to AChR of 1:1 to 2:1 [1]. AChR clustering is mediated by neural agrin that is released from the nerve terminal [2]. In early embryonic development, AChR clustering is also mediated by Wnt ligands [3,4]. Embryonic AChR is composed of α, β, δ, and γ subunits with a stoichiometry of $\alpha_2\beta\delta\gamma$. After birth, the ε subunit is substituted for the γ subunit, generating $\alpha_2\beta\delta\varepsilon$-AChR.

Congenital myasthenic syndromes (CMS) are heterogeneous disorders caused by mutations in genes expressed at the NMJ [5]. They are characterized by fatigable muscle weakness, variable muscle atrophy, and sometimes dysmorphic features. CMS mutations have been reported in 19 genes, with most mutations in *CHRNA1*, *CHRNB1*, *CHNRD*, and *CHNRE* encoding the AChR α, β, δ, and ε subunits, respectively. These mutations fall into three subsets: i) slow-channel CMS (SCCMS), in which the open time of AChR is abnormally prolonged; ii) fast-channel CMS (FCCMS), in which the open time of AChR is abnormally brief; and iii) endplate AChR deficiency. SCCMS is caused by a gain-of-function mutation and is dominantly inherited with variable penetrance [6]. In contrast, FCCMS and endplate AChR deficiency are caused by loss-of-function mutations on both alleles, and are recessively

* Corresponding author. Division of Neurogenetics, Center for Neurological Disease and Cancer, Nagoya University Graduate School of Medicine, 65 Tsurumai, Showa-ku, Nagoya 466-8550, Japan. Tel.: +81 52 744 2446; fax: +81 52 744 2449.
E-mail address: ohnok@med.nagoya-u.ac.jp (K. Ohno).

http://dx.doi.org/10.1016/j.nmd.2014.09.002
0960-8966/

inherited. Low-expressor mutations of the AChR ε subunit are partly compensated for by expression of the embryonic AChR γ subunit, whereas the other AChR subunits have no substituting subunits. Accordingly, null and frameshift mutations are frequently detected in *CHRNE*, but not in the other subunit genes.

More than 500 patients with CMS have been reported in Western and Middle Eastern countries, whereas only four Japanese CMS patients carrying five mutations in *COLQ* encoding collagen Q that anchors acetylcholinesterase (AChE) at the NMJ have been reported by us [7,8]. Among the more than 450 CMS mutations in 19 disease genes registered in the Human Gene Mutation Database (http://www.hgmd.org), two likely have founder effects: p.Asn88Lys in *RAPSN* [9–11] and c.1124_1127dupTGCC in *DOK7* [12], whereas the others are private mutations occurring in a single or a small number of unrelated families. We here report five Japanese CMS patients with six mutations in the AChR subunit genes. We show that all the ten mutations in *COLQ*, *CHRND*, and *CHRNE* in Japanese patients are ethnically unique, which indicates that most CMS mutations arose *de novo* in recent human history or in each family.

2. Materials and methods

2.1. Ethical approval

All the human studies were approved by the institutional review boards of Nagoya University Graduate School of Medicine, Mayo Clinic, Segawa Neurological Clinic for Children, Nagoya City University, and Tokyo Women's Medical University. Appropriate written informed consent was obtained from all the patients and family members.

2.2. Mutation analysis and splicing analysis

Genomic DNA was isolated from peripheral blood with QIAamp Blood Kit (QIAGEN). We directly sequenced all exons with their flanking noncoding regions of *CHRNE*, *CHRNA1*, *CHRNB1*, and *CHRND* in this order with CEQ 8000 (Beckman Coulter). To look for large-scale DNA rearrangements in patient (Pt.) 4, we performed mate-pair sequencing of the whole genome using SOLiD4 (Life Technologies). The mate-pair library was made to span ~2 kb genomic segments according to the manufacturer's protocols. A total of 14.9 Gb of reads were mapped to human genome GRCh37/hg19 with the mapping efficiency of 89% using CLC Genomics Workbench (CLC Bio). All the reads mapped to *CHRNE* were visually scrutinized using Integrative Genome Browser (Broad Institute). Total RNA was isolated from biopsied muscle that was obtained for histopathological diagnostic purposes using RNeasy mini kit (QIAGEN). cDNA was synthesized with ReverTra Ace (Toyobo) and Oligo(dT) Primer (Life Technologies).

2.3. Expression of AChR subunit genes in HEK293 cells

Human α, β, δ, and ε subunit cDNAs were cloned into the CMV-based vector pRBG4 for expression in HEK293 cells [13]. The identified mutations were engineered into wild-type AChR subunit cDNAs in pRBG4 using the QuikChange site-directed mutagenesis kit (Stratagene). Presence of each mutation and absence of unwanted artifacts were confirmed by sequencing the entire inserts. HEK293 cells were transfected with pRBG4-α, -β, -δ, -ε, and pcDNA3.1-EGFP at a ratio of 2:1:1:1:1 using FuGENE 6 transfection reagent (Promega). After 48 hrs, cells were incubated with α-bungarotoxin Alexa Flour 647 (Life Technologies) (1:200) in PBS for 1 hr. Signals were observed under an Olympus BX60 fluorescence microscope. The cells were trypsinized, washed with PBS, and resuspended in PBS. The total number of α-bungarotoxin-binding sites on the cell surface and EGFP was determined by the FACSCalibur system (BD Biosciences).

2.4. Single channel recordings

HEK293 cells were transfected with pRBG4-α, -β, -δ, and -ε, and pEGFP-N1 at a ratio of 2:1:1:1:1, using FuGENE 6. Recordings were obtained at 24 hrs after transfection in the cell-attached configuration at a membrane potential of –80 mV at 22 °C and with bath and pipette solutions containing (in mM): KCl, 142; NaCl, 5.4; CaCl2, 1.8; MgCl2, 1.7; HEPES, 10, pH 7.4. Single-channel currents were recorded using an Axopatch 200B amplifier (Axon Instruments) at a bandwidth of 50 kHz, digitized at 5-μs intervals using Digidata 1322A (Axon Instruments) and recorded to a hard disk using the program Clampex 8.2 (Axon Instruments). Recordings obtained with ACh at 1 μM or less were analyzed at a uniform bandwidth of 10–11.7 kHz with dead time of 15.3–17.9 μs imposed. Recordings obtained with ACh at 10 μM or more were analyzed with dead time at 25 μs at 10 kHz with TAC software (Ver. x4.0.9, Bruxton). Dwell-time histograms were plotted on a logarithmic abscissa and fitted by the sum of exponentials by maximum likelihood, as previously reported [14].

3. Results

3.1. Clinical features

All Pts. had an abnormal decremental response to repetitive nerve stimulation, and no anti-AChR and anti-MuSK antibodies. Clinical features and repetitive nerve stimulation results are summarized in Table 1.

Pt. 1 (13 y.o., male) had eyelid ptosis since age six months and a positive edrophonium test. Clinical features were previously reported in a local journal [15]. Steroid pulse therapy at ages four and five years and thymectomy at age six years had no effect. Combined use of distigmine 3 mg/day and pyridostigmine 180 mg/day enabled him to sit in a chair without assistance at age 13 years. Biopsy of deltoid muscle at age eleven years showed marked AChR deficiency by fluorescent staining with α-bungarotoxin and simplified endplates by electron microscopy.

Pt. 2 (26 y.o., female) had nasal obstruction since birth and eyelid ptosis since age one month. She had a positive edrophonium test and was thought to have myasthenia gravis. Cholinesterase inhibitors were mildly effective. She has ophthamoparesis, and is able to walk but is unable to run.

Table 1
Clinical features of six patients.

Pt.	Sex	Age	Onset	Consanguinity	Repetitive N. stimulation[a]	Drug[b]
1	M	13 y	6 m	–	Accessory N., 60%; Ulnar N., 53%	Distigmine 3 mg + pyridostigmine 180 mg, effective; 3,4-DAP 40 mg, mildly effective
2	F	26 y	1 m	+	Ulnar N., 80%	Pyridostigmine 150–180 mg, mildly effective
3	F	38 y	1 y	–	Ulnar N., 81%	Pyridostigmine 90–160 mg, moderately effective
4	F	6 y	2 y	–	Median N., 60%; Ulnar N., 68%	Pyridostigmine 90 mg + 3,4-DAP 30 mg, mildly effective; ephedrine 25 mg, effective
5	M	26 y	1 m	+	Ulnar N., 76%	Pyridostigmine 135 mg, moderately effective
6	M	11 y	Birth	–	Median N., 35%; Ulnar N., 31%	Prednisolone 35 mg *dieb. alt.*, effective

[a] Repetitive N. stimulation, repetitive nerve stimulation at 2–3 Hz. Relative amplitudes of the 5th CMAP are indicated. [b] Simultaneous prescription is indicated by "+".

Pt. 3 (38 y.o., female) had ptosis at age one year and was diagnosed to have myasthenia gravis at age seven years. Since then, she has been taking cholinesterase inhibitors and prednisolone, which seemed to help but could not climb steps after age 19 years.

Pt. 4 (6 y.o., female) walked alone at age 18 months, but since age two years she had repeated episodes of generalized muscle weakness that lasted about a week, especially when having a common cold. She could walk alone but was positive for a Gowers' sign. Cholinesterase inhibitors were moderately effective. Neurological examination of the mother detected no abnormality. The father was asymptomatic according to the mother, but was not examined by us. Clinical features were previously reported as patient 4 in a local journal [16].

Pt. 5 (26 y.o., male) had feeding difficulty at age one month and had eyelid ptosis since age five months. He has weak facial muscles and is unable to run. At age seven years, he had generalized muscle weakness during an upper respiratory infection. The edrophonium test was positive.

Pt. 6 (11 y.o., male) had repeated respiratory distress and respiratory infection during infancy. He walked alone at age one year, but was noticed to walk slowly at age five years with frequent falling episodes. Rest for a short time improved his walking, but there was no diurnal fluctuation of the symptoms. Intravenous administration of edrophonium chloride ameliorated walking difficulty, but long-acting cholinesterase inhibitors had no effect.

3.2. Mutation analysis

We directly sequenced AChR subunit genes in Pts. 1–6, and identified six mutations in *CHRND* and *CHRNE*, as well as a polymorphism in *CHRNB1* (Table 2). In this study, approved nucleotide and amino acid positions are used instead of the legacy annotation, in which nucleotide and amino acid positions start from the initiation sites of mature peptides.

Pt. 1 was compound heterozygous for c.1372-1G>A at the 3′ end of intron 11 of *CHRND* and c.127C>T predicting p.Arg44Trp at the extracellular domain of the δ subunit (Fig. 1A). cDNA extracted from biopsied muscle revealed that a newly generated 'ag' dinucleotide that was one nucleotide downstream of the native 'ag' was used as a splice acceptor site (Fig. 1B), which predicted p.Glu458Argfs*20 in the long cytoplasmic loop of the δ subunit (Fig. 1A). Pt. 2 was homozygous for c.655_665del predicting p.Gly219Argfs*7 in the extracellular domain of the ε subunit (Fig. 1A). Pt. 3 was heterozygous for p.Tyr262Ter in the M1 transmembrane domain of the ε subunit (Fig. 1A). Pt. 4 was heterozygous for p.Thr284Pro in the M2 transmembrane domain of the ε subunit (Fig. 1A). Pt. 5 was homozygous for p.Leu304Arg in the short extracellular link between the M2 and M3 transmembrane domains of the ε subunit (Fig. 1A). Pt. 6 was heterozygous for p.Met465Thr close to the C-terminal end of the long cytoplasmic loop connecting the M3 and M4 transmembrane domains of AChR β subunit (Fig. 1A).

Table 2
Six mutations and one polymorphism identified in AChR subunit genes.

Pt.	Gene	Nucleotide change[c]	Amino-acid change[c]	Legacy annotation[d]	Phenotypic consequence
1	*CHRND*	c.1372-1G>A	δp.Glu458Argfs*20	δE437fs	AChR deficiency
	CHRND	c.127C>T	δp.Arg44Trp	δR23W	AChR deficiency
2[a]	*CHRNE*	c.655_665del	εp.Gly219Argfs*7	εG199fs	AChR deficiency
3[b]	*CHRNE*	c.786C>G	εp.Tyr262Ter	εY242X	AChR deficiency
4	*CHRNE*	c.850A>C	εp.Thr284Pro	εT264P	SCCMS
5[a]	*CHRNE*	c.911T>G	εp.Leu304Arg	εL284R	AChR deficiency
6	*CHRNB1*	c.1394T>C	εp.Met465Thr	βM442T	~50% shortening of AChR openings

[a] Patient is homozygous for the mutation.
[b] A mutation on another allele remains unidentified.
[c] Nucleotide and amino acid positions start from the translational start sites.
[d] In legacy annotation, nucleotide and amino acid positions start from the initiation sites of mature peptides, which are 69 nt. (23 amino acids), 63 nt. (21 amino acids), and 60 nt. (20 amino acids) downstream of the translational start sites of *CHRNB1*, *CHRND*, and *CHRNE*, respectively.

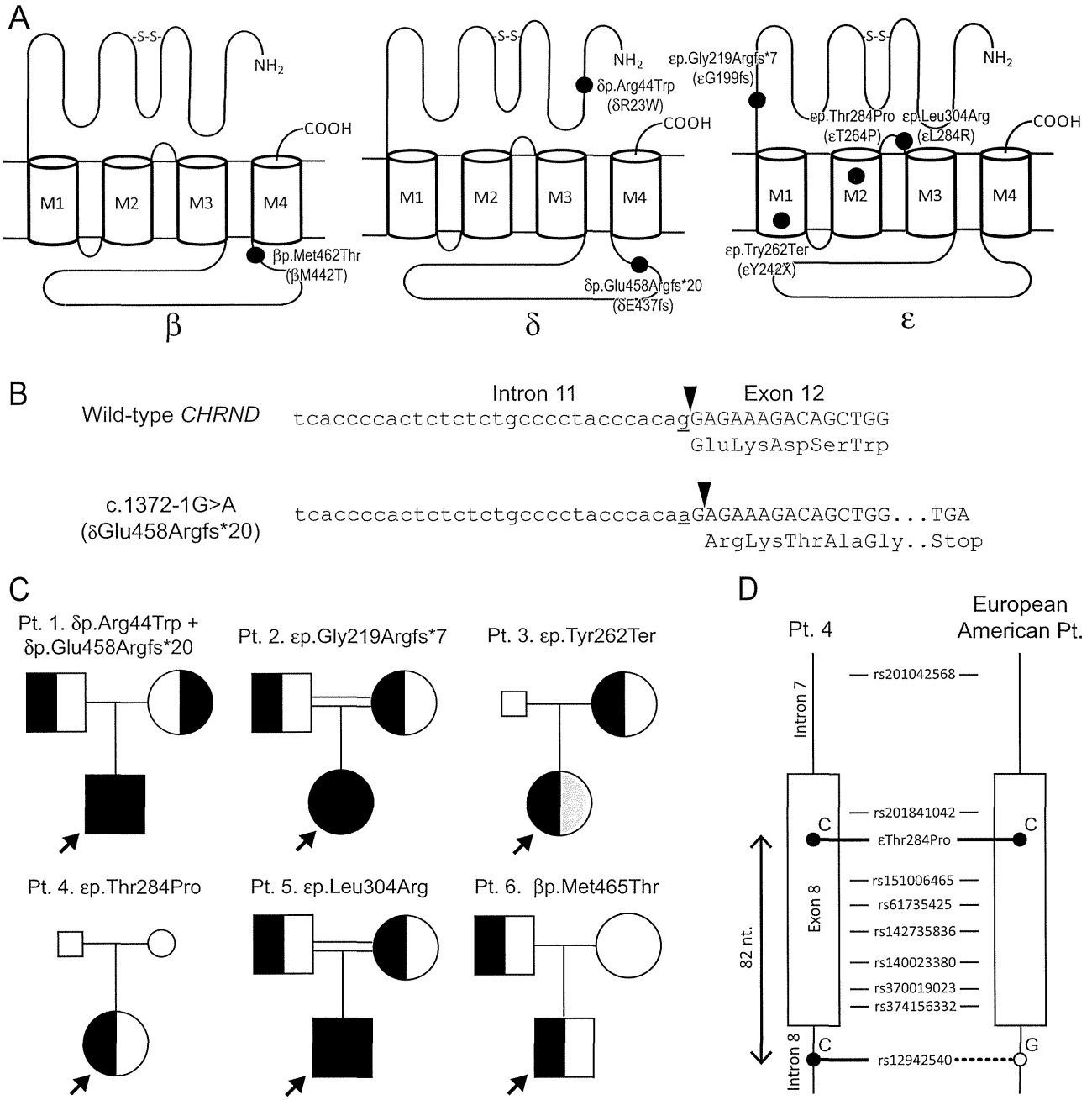

Fig. 1. Six mutations and a single polymorphism in AChR subunit genes identified in six CMS patients. (A) Positions of six mutations and a polymorphism. M1-M4, the first to fourth transmembrane domains. The M2 domains form a channel pore of AChR. (B) RT-PCR of biopsied muscle of Pt. 1 reveals that c.1372-1G>A (underlined) shifts a splice acceptor site (arrowheads) one nucleotide downstream, which predicts a shift in the reading frame (δp.Glu458Argfs*20). (C) Pedigree analyses of the mutations. Patients are indicated by arrows. Full and half shaded symbols represent homozygous and heterozygous mutations, respectively. Gray half shaded symbols represent that the individuals are predicted to carry a heterozygous mutation, the identity of which, however, has not been identified. Small symbols indicate that DNA is not available. (D) Haplotype analysis of εp.Thr284Pro in Pt. 4 and the previously reported European American Pt [7]. Both patients carry discordant nucleotides at rs12942540, which is 82 nt. downstream of the mutation.

δp.Arg44Trp (rs55868108) in Pt. 1 was previously reported in one of five healthy controls, but its ethnic origin was not documented [17]. δp.Arg44Trp, however, is not observed in the 1000 genome project (http://www.1000genomes.org/) or in the human gene variation database (HGVD), which collates SNPs in a large cohort of Japanese individuals (http://www.genome.med.kyoto-u.ac.jp/SnpDB/) [18]. As indicated below, functional analysis disclosed that δp.Arg44Trp

Table 3
Open intervals and bursts of wild-type and mutant AChR expressed on HEK cells.

	Open intervals		Bursts	
	Wild-type	βp.Met465Thr	Wild-type	βp.Met465Thr
τ_1 (ms)	0.037 ± 0.0033[a]	0.022[b]	0.036 ± 0.0017[c]	0.039 ± 0.006[d]
(a_1)	(0.17 ± 0.022)	(0.18)	(0.24 ± 0.021)	(0.18 ± 0.034)
τ_2 (ms)	0.31 ± 0.050	0.16 ± 0.017[e]	0.47 ± 0.059	0.16 ± 0.037[f]
(a_2)	(0.27 ± 0.038)	(0.23 ± 0.031)	(0.21 ± 0.027)	(0.23 ± 0.010)
τ_3 (ms)	1.35 ± 0.051	0.98 ± 0.034	3.31 ± 0.12	1.93 ± 0.085
(a_3)	(0.67 ± 0.042)	(0.78 ± 0.028)	(0.58 ± 0.038)	(0.82 ± 0.034)

Twenty-one wild-type and seven mutant patches were analyzed. Time constants, τ_n, and fractional areas, a_n, for each component are presented with mean ± SEM. ACh concentration was 50–100 nM.
[a–f] Not detected at 12, 6, 3, 5, 1, and 3 patches, respectively.
Final band widths were 11.7 and 10 kHz for wild-type and mutant AChRs, respectively.

significantly reduces cell surface expression of AChR and is unlikely to be polymorphism.

p.Met465Thr (rs201776800) in Pt. 6 was observed in eight alleles in eight Japanese individuals in the 1000 genome project with a minor allelic frequency (MAF) of 0.004, as well as in 119 alleles in a cohort of 1170 Japanese individuals in HGVD with a MAF of 0.051. Although p.Met465Thr was likely to be a polymorphism according to the high MAFs in the Japanese, we scrutinized functional consequences of p.Met465Thr in this study.

*3.3. εp.Gly219Argfs*7, εp.Tyr262Ter, and δp.Glu458Argfs*20 are predicted to compromise AChR expression*

Among the six mutations, εp.Gly219Argfs*7 in Pt. 2 and εp.Tyr262Ter in Pt. 3 were predicted to produce truncated ε subunits. We previously reported that truncation mutations in the εsubunit lead to expression of the embryonic $\alpha_2\beta\delta\gamma$-AChR at the patient's endplates and the patients have endplate AChR deficiency [19–21]. The ε mutations in Pts. 2 and 3 were thus predicted to cause AChR deficiency.

δp.Glu458Argfs*20 in Pt. 1 was predicted to generate a truncated δ subunit that cannot be incorporated into mature AChR. The phenotype of Pt. 1 is thus determined by δp.Arg44Trp on the other allele, which causes AChR deficiency as indicated below.

3.4. εp.Thr284Pro is an established slow-channel mutation without shared haplotype with a European American patient

εp.Thr284Pro in the M2 domain of the ε subunit was identical to the first characterized slow-channel mutation reported in a patient of Swiss and Turkish descent [22]. We asked if the mutation in Pt. 4 derived from the same founder allele as the first reported patient. Therefore we sequenced exon 8 and its flanking intronic regions where nine SNPs were located (Fig. 1C). This revealed that the mutant allele in the Japanese patient had 'C', whereas the mutant allele in the European American patient had 'G' at rs12942540 in intron 8, which was located 82 nt. downstream of εp.Thr284Pro. Accordingly, εp.Thr284Pro in both patients is likely to have occurred independently in two ethnic groups.

3.5. δp.Arg44Trp and εp.Leu304Arg, but not βp.Met465Thr, decrease cell surface expression of AChR in transfected HEK293 cells

We next analyzed the effects of AChR expression of the remaining three mutations of δp.Arg44Trp, εp.Leu304Arg and βp.Met465Thr. We introduced wild-type or mutant α, β, δ, and ε subunit cDNAs along with EGFP cDNA into HEK293 cells (Fig. 2A), and measured cell surface expression of AChR detected by Alexa 647-labeled α-bungarotoxin using FACS. Expression of βp.Met465Thr-AChR was similar to that of wild-type AChR, whereas δp.Arg44Trp and εp.Leu304Arg markedly attenuated the cell surface expression of AChR (Figs. 2B and C). Accordingly, δp.Arg44Trp and εp.Leu304Arg cause endplate AChR deficiency.

3.6. βp.Met465Thr mildly shortens channel opening events, but not as much as the other established fast channel mutations

As βp.Met465Thr-AChR was efficiently expressed on HEK293 cells, we next recorded opening and closing of single AChR channels at limiting low concentrations of ACh by the patch clamp method (Fig. 3A). We found that the major burst duration (τ_3) was decreased from 3.31 ms to 1.93 ms (58.3%) in βp.Met465Thr-AChR (Table 3), while the conductance of βp.Met465Thr-AChR was normal. Distributions of opening probabilities of the clusters generated by 10 μM or greater concentrations of ACh made single peaks for both wild-type and mutant AChRs. Thus, βMet465Thr mildly shortens the channel openings but does not cause a mode switching in the kinetics of the receptor activation, which is seen in other FCCMS mutations [23,24].

3.7. A recessive mutation on the other allele in Pt. 3 remains unidentified

Functional prediction and characterization of the six mutations indicated that εp.Thr284Pro in Pt. 4 was a dominant slow-channel mutation [22], whereas the other five mutations in Pts. 1, 2, 3, and 5 were recessive loss-of-function mutations. The mutations in Pts. 1, 2, and 5 were biallelic, whereas a mutation was detected only on a single allele in Pt. 3 (Fig. 1C).

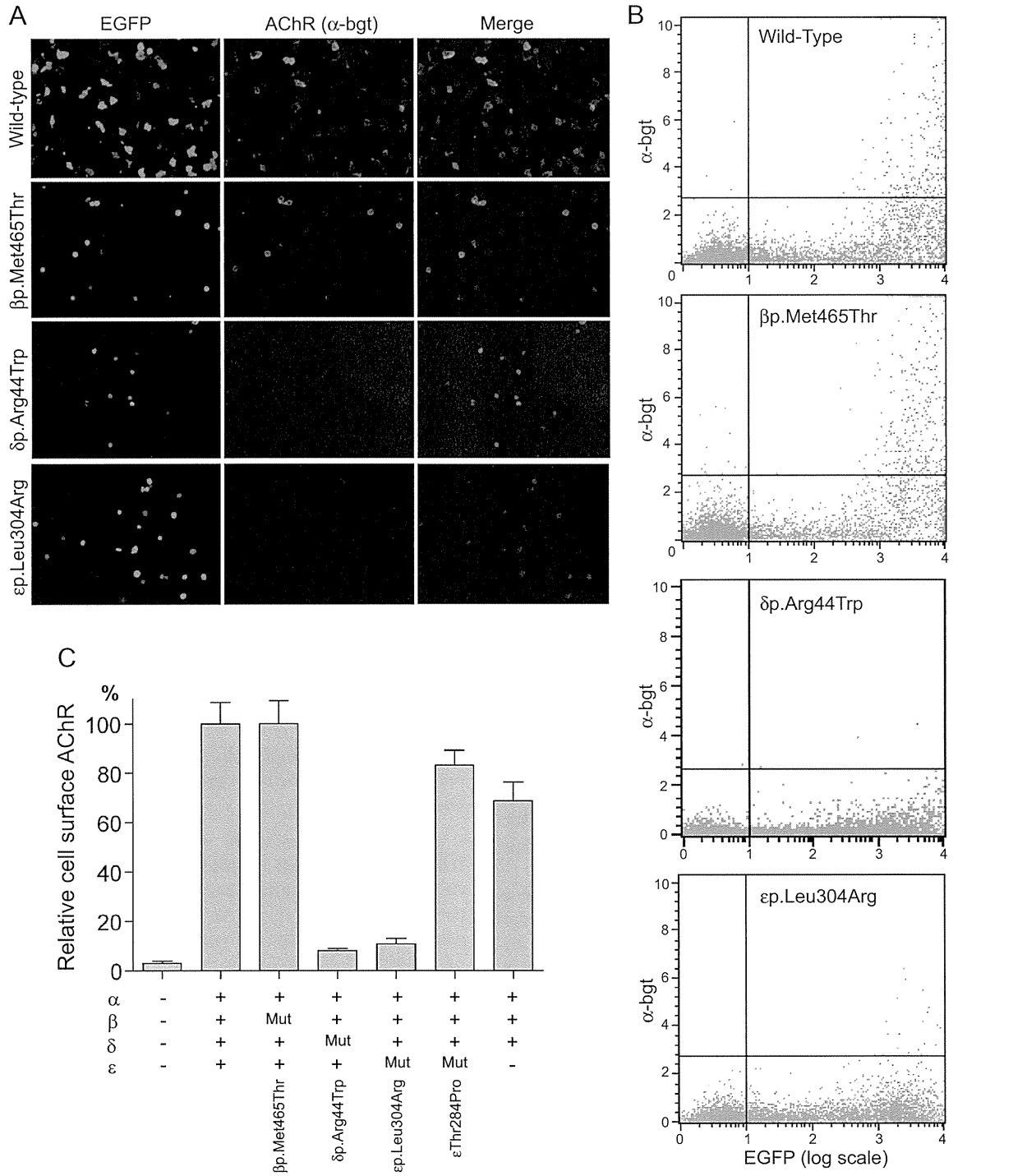

Fig. 2. Quantification of cell surface expression of wild-type and mutant AChRs on HEK293 cells. (A) HEK293 cells are transfected with wild-type or mutant AChR subunit cDNAs along with EGFP cDNA. Only transfected cells have EGFP signals and AChRs that are visualized with Alexa 647-labeled α-bungarotoxin (bgt). εp.Leu304Arg-AChR has less signals for AChRs compared to wild-type and βp.Met465Thr-AChRs. (B) Representative FACS profiles of EGFP and Alexa 647-labeled α-bgt. Both axes are shown in arbitrary units. The number of cells fractioned into the upper right quadrant is counted as AChR-positive cells. (C) Ratios of AChR-positive cells (the upper right quadrant) divided by EGFP-positive cells (the lower right quadrant). δp.Arg44Trp and εp.Leu304Arg markedly decrease AChR expression, whereas βp.Met465Thr and εp.Thr284Pro have no effect on AChR expression. ε-deficient $\alpha_2\beta\delta_2$-AChR are expressed at ~70% of wild-type, as we reported previously [21]. Mut, a mutant AChR subunit. Mean and SE are indicated ($n = 12$).

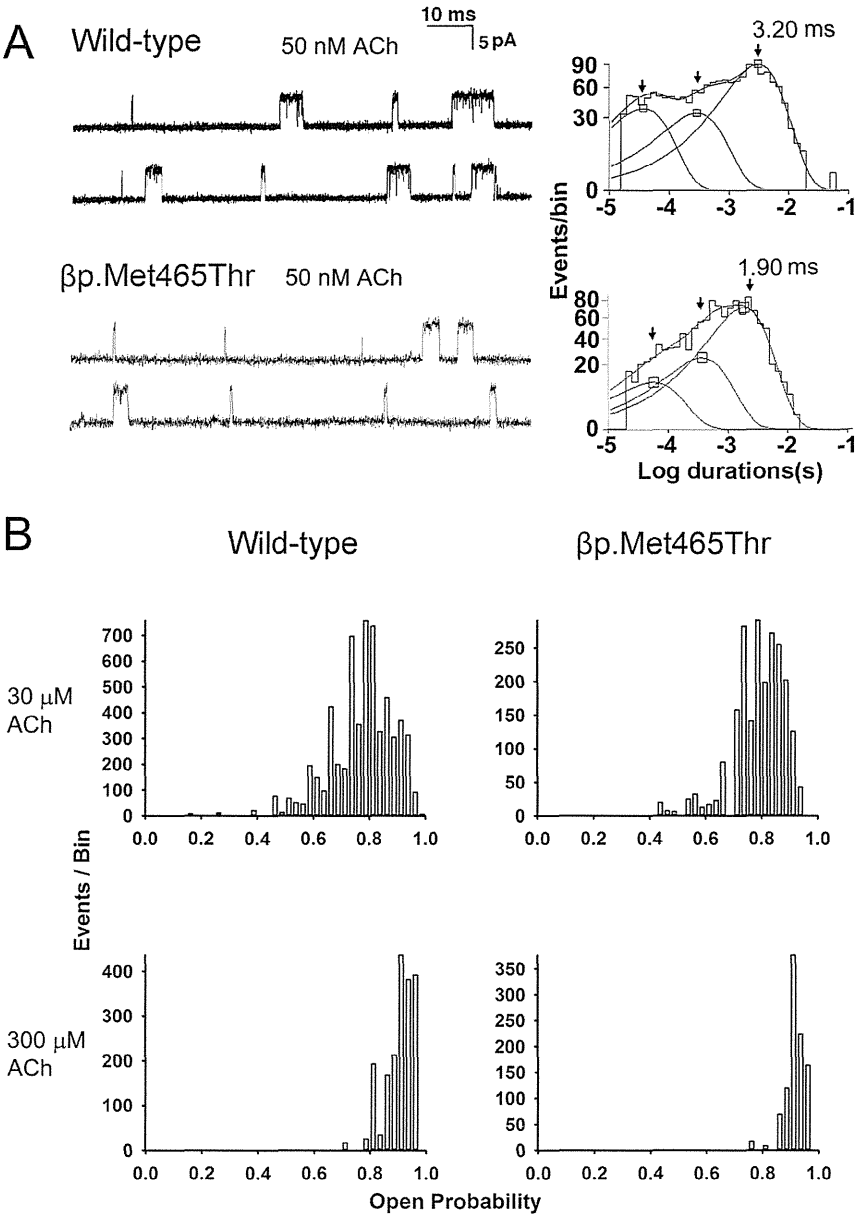

Fig. 3. Single channel currents of wild-type and mutant AChRs on HEK293 cells. (A) Left: Representative channel openings shown as upward deflections. Right: Burst duration histograms fitted to the sum of exponentials. Arrows indicate mean durations of dominant burst components. (B) Distribution of open probabilities from individual clusters obtained at the indicated ACh concentrations. Note that both wild-type and mutant AChRs make a single peak.

We scrutinized all exonic nucleotides in *CHRNE* in Pt. 3 by bidirectional sequencing, but detected none. We therefore hypothesized that a mutation on the other alleles was either a promoter mutation, a splice-site mutation disrupting a deep intronic splicing *cis*-element, or a large-scale DNA rearrangement. Sequencing of ~1 kb upstream of the translation initiation sites, however, revealed no mutation. We further analyzed genomic DNA by mate-pair sequencing of the whole genome. A total of 57 reads were mapped to *CHRNE*. Visual inspection of these reads, however, failed to detect any large-scale DNA rearrangements or any mutations. A recessive mutation on the other allele in *CHRNE* in Pt. 3 thus remains unidentified. We also analyzed 18 other CMS-causing genes using the mate-pair sequencing data in Pt. 3. As the mate-pair sequencing was for detecting a large-scale DNA rearrangement, the 18 genes were covered by only 10,116 reads. Although the coverage was not high enough for detecting SNVs, no candidate mutations were detected in Pt. 3.

Table 4
Fifteen previously reported FCCMS mutations and the currently analyzed βp.Met462Thr polymorphism.

Mutation	Burst duration (ms)			Expression	Domain	Reference
	Wild-type	Mutant	Ratio	(%)		
αp.Val152Leu (αV132L)	3.31	0.50	0.151	135	Extracellular domain of α	[25]
αp.Val208Met (αV188M)	3.31	0.68	0.205	90	Extracellular domain of α	[26]
αp.Phe276Leu (αF256L)	3.62	0.30	0.083	102	M2 domain of α	[27]
αp.Val305Ile (αV285I)	2.99	0.34	0.114	116	M3 domain of α	[28]
δp.Leu63Pro (δL42P)	3.31	0.18	0.054	37	Extracellular domain of δ	[14]
δp.Glu80Lys (δE59K)	5.06	2.75	0.543	62	Extracellular domain of δ	[29]
δp.Pro271Gln (δP250Q)	3.31	1.54	0.465	60	M1 domain of δ	[30]
εp.Thr58Lys (εT38K)	5.86	0.06	0.010	78	Extracellular domain of ε	[31]
εp.Trp75Arg (εW55R)	3.31	0.37	0.112	86	Extracellular domain of ε	[32]
εp.Pro141Leu (εP121L)	2.99	0.45	0.151	102	Extracellular domain of ε	[13]
εp.Asp195Asn (εD175N)	2.13	0.49	0.230	117[b]	Extracellular domain of ε	[33]
εp.Asn202Tyr (εN182Y)	2.13	0.65	0.305	117[b]	Extracellular domain of ε	[33]
εp.Ser433_Glu438dup (ε1254ins18)	2.80	1.01	0.361	47	Long cytoplasmic loop of ε	[23]
εp.Ala431Pro (εA411P)	n.a.[a]	n.a.[a]	n.a.[a]	31	Long cytoplasmic loop of ε	[24]
εp.Asn456del (εN436del)	3.31	1.24	0.375	51	Long cytoplasmic loop of ε	[34]
βp.Met462Thr (βM442T)	3.31	1.93	0.583	99	Long cytoplasmic loop of β	Current study

A major component of burst durations of wild-type and mutant AChRs expressed in HEK293 cells is indicated. Cell surface expression in HEK293 cells is normalized to that of wild-type. Channel openings are elicited by 50–100 nM ACh. Mutations in parentheses are legacy annotations used in original reports.

[a] Detailed ion channel kinetics are analyzed using a hidden Markov model, but burst durations are not indicated.

[b] Cell surface expression of recombinant AChR is not indicated, and the expression ratio is calculated from α-bungarotoxin binding sites of control and patient endplates.

4. Discussion

We identified six mutations in AChR subunit genes in five Japanese patients with CMS. We initially assumed that βp.Met465Thr in Pt. 6 was a mild fast-channel mutation. However, expansion of the SNP database later disclosed that βp.Met465Thr is a polymorphism that is frequently observed in the Japanese population. Fifteen previously reported FCCMS mutations shorten burst durations to 22.6 ± 16.1% of wild-type (mean and SD; range 1.0%–54.3%) (Table 4). A FCCMS mutation, δp.Glu80Lys (δE59K), decreases burst durations to 54.3% of wild-type [29], which is similar to 58.3% observed in the current βp.Met465Thr polymorphism. However, in contrast to βp.Met465Thr, δp.Glu80Lys reduces cell surface expression of AChR to 62% of wild-type [29]. Similarly, δp.Pro271Gln (δP250Q) mildly reduces burst durations to 46.5% of wild-type, but again, unlike βp.Met465Thr, this mutation reduces cell surface expression of AChR to 60% of wild-type [30]. A plot of normalized burst durations and normalized cell surface expressions suggests that a mean burst duration of less than ~30% causes FCCMS even when it does not affect the cell surface expression of AChR (Fig. 4). In contrast, a mean burst duration of between ~30% and ~60% causes FCCMS when the mutation reduces the cell surface expression of AChR to ~60% or less (Fig. 4). However, as no individual is homozygous for βp.Met465Thr or carries a null mutation on the other allele, pathogenicity of βp.Met465Thr in the absence of a normal *CHRND* on the other allele still remains unknown.

δp.Arg44Trp is close to the N-terminal end of the extracellular region (Fig. 5). We previously reported that a similar εp.Arg40Trp also causes AChR deficiency [35]. The specific function of this region, however, is not well dissected. εp.Leu304Arg is in the short extracellular link between the M2 and M3 transmembrane domains (Fig. 5). The functions of this link are not well characterized. In this link, only αp.Ser289Ile (αS269I) is reported in SCCMS [38]. βp.Met465Thr is located close to the C-terminal end of the long cytoplasmic loop that links the M3 and M4 transmembrane domains (Fig. 5). Interestingly, three FCCMS mutations in the long cytoplasmic loop are clustered close to the C-terminal end of the ε subunit [23,24,34,36,37], and similarly destabilize the channel open state. Two FCCMS mutations in this region, εp.Ser433_Glu438dup (ε1254ins18) [23] and εp.Ala431Pro (εA411P) [24], disrupt the fidelity of gating and result in unstable channel kinetics. In addition, another FCCMS

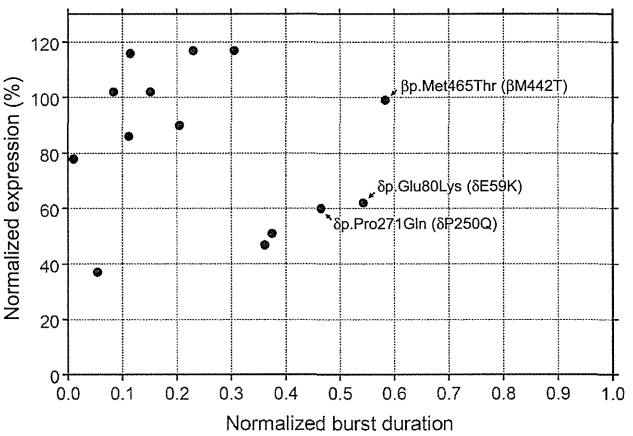

Fig. 4. Normalized burst durations and normalized cell surface expressions of previously reported FCCMS mutations and the currently analyzed βp.Met462Thr polymorphism shown in Table 4. Arrows point to mutations and a polymorphism that are addressed in the discussion.

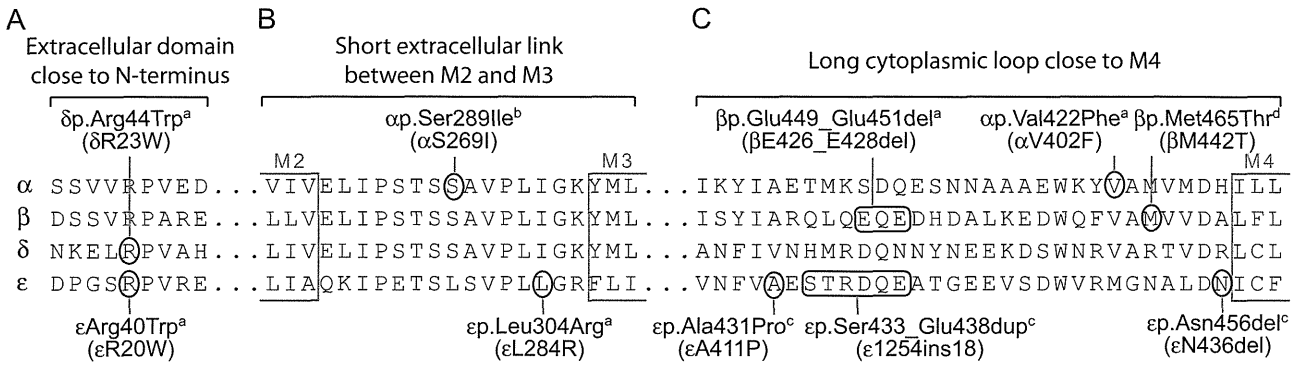

Fig. 5. Positions of the currently identified δp.Arg44Trp, εp.Leu304Arg and βp.Met465Thr, as well as previously reported CMS mutations. Mutations in the extracellular domain close the N-terminal end (A), the short extracellular link between the M2 and M3 transmembrane domains (B), and the long cytoplasmic loop close to the M4 transmembrane domain (C) are indicated. [a]δp.Arg44Trp (current report), εp.Arg40Trp [35], βp.Glu449_Glu451del [36], and αp.Val422Phe [37] cause AChR deficiency (AChR def.). [b]αp.Ser289Ile [38] causes SCCMS. [c]εp.Ala431Pro [24], ε p.Ser433_Glu438dup [23], and εp.Asn456del [34] cause FCCMS. [d]βp.Met465Thr is a currently analyzed polymorphism that shortens channel opening events. Mutations in parentheses are legacy annotations used in the original reports.

mutation in this region, εp.Asn456del (εN436del), destabilizes the diliganded receptor [34]. The C-terminal region of the long cytoplasmic loop of the ε subunit is thus likely to be crucial for stabilizing the open channel. In contrast to the three FCCMS mutations in the C-terminal end, however, βp.Met465Thr mildly shortens channel opening events and has no effect on the fidelity of channel gating, which may represent subunit-specificity and/or position-specificity of the amino acid substitutions.

Excluding δp.Arg44Trp that was previously reported in a healthy subject of unknown ethnicity [17], five of the six mutations in the AChR subunit genes in the current study and the five previously identified *COLQ* mutations [8] are unique to Japanese people. This is in contrast to some CMS mutations that are observed in unrelated families in Western and Middle Eastern countries. Especially, founder effects are implicated in two mutations: p.Asn88Lys in *RAPSN* [9–11] and c.1124_1127dupTGCC in *DOK7* [12]. CMS mutations are all recessively inherited except for those causing SCCMS. As heterozygous carriers of recessive CMS mutations exhibit no clinical phenotypes even by detailed electrophysiological studies, an asymptomatic carrier of a recessive CMS mutation has no disadvantage in transmitting the mutant allele to offspring. Lack of founder effects between the Japanese patients and patients of other nationalities thus suggest that most but not all CMS mutations arose *de novo* in a recent human history or in each family.

Acknowledgments

This study was supported by Grants-in-Aid from the MEXT and MHLW of Japan to KO. We would like to thank Dr. Andrew G. Engel for critical and constructive discussion on this project.

References

[1] Borges LS, Yechikhov S, Lee YI, et al. Identification of a motif in the acetylcholine receptor beta subunit whose phosphorylation regulates rapsyn association and postsynaptic receptor localization. J Neurosci 2008;28:11468–76.
[2] Bezakova G, Ruegg MA. New insights into the roles of agrin. Nat Rev Mol Cell Biol 2003;4:295–308.
[3] Budnik V, Salinas PC. Wnt signaling during synaptic development and plasticity. Curr Opin Neurobiol 2011;21:151–9.
[4] Korkut C, Budnik V. WNTs tune up the neuromuscular junction. Nat Rev Neurosci 2009;10:627–34.
[5] Ohno K, Ito M, Engel AG. Congenital myasthenic syndromes – molecular bases of congenital defects of proteins at the neuromuscular junction. In: Zaher A, editor. Neuromuscul. Disord. Rijeka: InTech; 2012. p. 175–200.
[6] Croxen R, Hatton C, Shelley C, et al. Recessive inheritance and variable penetrance of slow-channel congenital myasthenic syndromes. Neurology 2002;59:162–8.
[7] Ohno K, Engel AG, Brengman JM, et al. The spectrum of mutations causing endplate acetylcholinesterase deficiency. Ann Neurol 2000;47:162–70.
[8] Nakata T, Ito M, Azuma Y, et al. Mutations in the C-terminal domain of ColQ in endplate acetylcholinesterase deficiency compromise ColQ-MuSK interaction. Hum Mutat 2013;34:997–1004.
[9] Ohno K, Engel AG. Lack of founder haplotype for the rapsyn N88K mutation: N88K is an ancient founder mutation or arises from multiple founders. J Med Genet 2004;41:e8.
[10] Muller JS, Abicht A, Burke G, et al. The congenital myasthenic syndrome mutation RAPSN N88K derives from an ancient Indo-European founder. J Med Genet 2004;41:e104.
[11] Dunne V, Maselli RA. Common founder effect of rapsyn N88K studied using intragenic markers. J Hum Genet 2004;49:366–9.
[12] Ben Ammar A, Petit F, Alexandri N, et al. Phenotype genotype analysis in 15 patients presenting a congenital myasthenic syndrome due to mutations in DOK7. J Neurol 2010;257:754–66.
[13] Ohno K, Wang HL, Milone M, et al. Congenital myasthenic syndrome caused by decreased agonist binding affinity due to a mutation in the acetylcholine receptor epsilon subunit. Neuron 1996;17:157–70.
[14] Shen XM, Fukuda T, Ohno K, Sine SM, Engel AG. Congenital myasthenia-related AChR delta subunit mutation interferes with intersubunit communication essential for channel gating. J Clin Invest 2008;118:1867–76.
[15] Ishigaki K, Murakami T, Ito Y, et al. [Treatment approach to congenital myasthenic syndrome in a patient with acetylcholine receptor deficiency]. No to Hattatsu 2009;41:37–42.
[16] Irahara K, Komaki H, Honda R, et al. [Clinical features of congenital myasthenic syndrome in Japan]. No to Hattatsu 2012;44:450–4.
[17] Denning L, Anderson JA, Davis R, Gregg JP, Kuzdenyi J, Maselli RA. High throughput genetic analysis of congenital myasthenic syndromes using resequencing microarrays. PLoS ONE 2007;2:e918.

[18] Narahara M, Higasa K, Nakamura S, et al. Large-scale East-Asian eQTL mapping reveals novel candidate genes for LD mapping and the genomic landscape of transcriptional effects of sequence variants. PLoS ONE 2014;9:e100924.
[19] Engel AG, Ohno K, Bouzat C, Sine SM, Griggs RC. End-plate acetylcholine receptor deficiency due to nonsense mutations in the epsilon subunit. Ann Neurol 1996;40:810–17.
[20] Engel AG, Ohno K, Milone M, et al. New mutations in acetylcholine receptor subunit genes reveal heterogeneity in the slow-channel congenital myasthenic syndrome. Hum Mol Genet 1996;5:1217–27.
[21] Ohno K, Quiram PA, Milone M, et al. Congenital myasthenic syndromes due to heteroallelic nonsense/missense mutations in the acetylcholine receptor epsilon subunit gene: identification and functional characterization of six new mutations. Hum Mol Genet 1997;6:753–66.
[22] Ohno K, Hutchinson DO, Milone M, et al. Congenital myasthenic syndrome caused by prolonged acetylcholine receptor channel openings due to a mutation in the M2 domain of the epsilon subunit. Proc Natl Acad Sci U S A 1995;92:758–62.
[23] Milone M, Wang H-L, Ohno K, et al. Mode switching kinetics produced by a naturally occurring mutation in the cytoplasmic loop of the human acetylcholine receptor epsilon subunit. Neuron 1998;20:575–88.
[24] Wang H-L, Ohno K, Milone M, et al. Fundamental gating mechanism of nicotinic receptor channel revealed by mutation causing a congenital myasthenic syndrome. J Gen Physiol 2000;116:449–62.
[25] Shen X-M, Ohno K, Tsujino A, et al. Mutation causing severe myasthenia reveals functional asymmetry of AChR signature cystine loops in agonist binding and gating. J Clin Invest 2003;111:497–505.
[26] Shen XM, Brengman JM, Sine SM, Engel AG. Myasthenic syndrome AChRalpha C-loop mutant disrupts initiation of channel gating. J Clin Invest 2012;122:2613–21.
[27] Webster R, Brydson M, Croxen R, Newsom-Davis J, Vincent A, Beeson D. Mutation in the AChR ion channel gate underlies a fast channel congenital myasthenic syndrome. Neurology 2004;62:1090–6.
[28] Wang H-L, Milone M, Ohno K, et al. Acetylcholine receptor M3 domain: stereochemical and volume contributions to channel gating. Nat Neurosci 1999;2:226–33.
[29] Brownlow S, Webster R, Croxen R, et al. Acetylcholine receptor d subunit mutations underlie a fast-channel myasthenic syndrome and arthrogryposis multiplex congenita. J Clin Invest 2001;108:125–30.
[30] Shen XM, Ohno K, Fukudome T, et al. Congenital myasthenic syndrome caused by low-expressor fast-channel AChR delta subunit mutation. Neurology 2002;59:1881–8.
[31] Webster R, Liu WW, Chaouch A, Lochmuller H, Beeson D. Fast-channel congenital myasthenic syndrome with a novel acetylcholine receptor mutation at the alpha-epsilon subunit interface. Neuromuscul Disord 2014;24:143–7.
[32] Shen XM, Brengman JM, Edvardson S, Sine SM, Engel AG. Highly fatal fast-channel syndrome caused by AChR epsilon subunit mutation at the agonist binding site. Neurology 2012;79:449–54.
[33] Sine SM, Shen X-M, Wang H-L, et al. Naturally occurring mutations at the acetylcholine receptor binding site independently alter ACh binding and channel gating. J Gen Physiol 2002;120:483–96.
[34] Shen XM, Ohno K, Sine SM, Engel AG. Subunit-specific contribution to agonist binding and channel gating revealed by inherited mutation in muscle acetylcholine receptor M3-M4 linker. Brain 2005;128:345–55.
[35] Shen X-M, Ohno K, Milone M, Brengman JM, Spilsbury P, Engel AG Low-affinity fast-channel syndrome. Neurology 2001;56(Suppl. 3):A60. (abstract).
[36] Quiram PA, Ohno K, Milone M, et al. Mutation causing congenital myasthenia reveals acetylcholine receptor beta/delta subunit interaction essential for assembly. J Clin Invest 1999;104:1403–10.
[37] Milone M, Shen X-M, Ohno K, et al. Unusual congenital myasthenic syndrome with endplate AChR deficiency caused by alpha subunit mutations and a remitting-relapsing clinical course. Neurology 1999;51(Suppl. 2):A185. (abstract).
[38] Croxen R, Newland C, Beeson D, et al. Mutations in different functional domains of the human muscle acetylcholine receptor alpha subunit in patients with the slow-channel congenital myasthenic syndrome. Hum Mol Genet 1997;6:767–74.